23. Our time scale is based on a carbon cycling model that assumes that a steady removal of light carbon from the oceans and atmosphere will occur after an initial input of isotopically negative $\delta^{13}C$. Reequilibration of the ocean $\delta^{13}C$ signature will occur in an exponential fashion, according to published equations (*30*). The general shape of our $\delta^{13}C$ records suggests that this mechanism is at work during the LPTM and hence provides us with an independent first-order estimate of time. Because the residence time of carbon is ~100,000 years (also referred to as the e-folding time), it is possible to deduce the duration of small-scale events within the CIE by close examination of our records. After two e-folding times, the CIE signal should be reduced to within ~14% of its pre-excursion levels. We have estimated this ~200,000-year interval in Fig. 2 while taking into account the extended duration of methane injection and the negative $\delta^{13}C$ trend that persists well into the Early Eocene. The onset of the CIE is assigned an age of 55.5 million years ago (*20*), which coincides precisely with the BEE in both sites. We assumed constant sedimentation rates before, during, and after the CIE.
24. R. M. Corfield and R. D. Norris, in *Late Paleocene–Early Eocene Climatic and Biotic Events in the Marine and Terrestrial Records*, M.-P. Aubry, S. G. Lucas, W. A. Berggren, Eds. (Columbia Univ. Press, New York, 1998), pp. 124–137.
25. E. Thomas, *Proc. Ocean Drilling Prog. Sci. Results* **113**, 571 (1990).
26. T. F. Stocker and A. Schmittner, *Nature* **388**, 862 (1997)
27. R. M. Corfield, *Earth Sci. Rev.* **37**, 225 (1994).
28. J. S. Booth, W. J. Winters, W. P. Dillon, M. B. Clennell, M. M. Rowe, in (*15*), pp. 113–128.; G. D. Ginsburg, in (*15*), pp. 61–62.; B. U. Haq, in *Gas Hydrates*, J.-P. Henriet and J. Mienert, Eds. (Geological Society, London, 1998), pp. 303–318.
29. One gigaton = 1×10^{15} g.
30. W. H. Berger and E. Vincent, *Geol. Rundsch.* **75**, 249 (1986).
31. N. J. Shackleton, in *Fossils and Climate*, P. J. Brenchley, Ed. (Wiley, New York, 1984), pp. 27–34.
32. We thank J. Cartlidge and S. Wyatt for their expert help in the operation of the mass spectrometers in the Stable Isotope Laboratory at Oxford and O. Green, D. Patrick, W. Hale, M. Bowman, P. Weiss, and J. Firth for assistance. This work was supported by the Natural Environment Research Council (U.K.), scholarship number GT4/97/214/ES.

29 March 1999; accepted 28 May 1999

Activation of NK Cells and T Cells by NKG2D, a Receptor for Stress-Inducible MICA

Stefan Bauer,[1*†] Veronika Groh,[1*] Jun Wu,[2] Alexander Steinle,[1] Joseph H. Phillips,[2] Lewis L. Lanier,[2] Thomas Spies[1‡]

Stress-inducible MICA, a distant homolog of major histocompatibility complex (MHC) class I, functions as an antigen for γδ T cells and is frequently expressed in epithelial tumors. A receptor for MICA was detected on most γδ T cells, $CD8^+$ αβ T cells, and natural killer (NK) cells and was identified as NKG2D. Effector cells from all these subsets could be stimulated by ligation of NKG2D. Engagement of NKG2D activated cytolytic responses of γδ T cells and NK cells against transfectants and epithelial tumor cells expressing MICA. These results define an activating immunoreceptor-MHC ligand interaction that may promote antitumor NK and T cell responses.

Major histocompatibility complex class I molecules are ligands for inhibitory or activating natural killer (NK) cell receptors that are expressed on NK cells and T cells. These include isoforms of the immunoglobulin (Ig)-like killer cell receptors that interact with HLA-A, -B, or -C, and CD94 paired with NKG2A or NKG2C, which bind HLA-E (*1–4*). Engagement of these receptors modulates NK cell responses and T-cell antigen receptor (TCR)-dependent T-cell activation (*1, 5*).

Expression of MHC class I is frequently impaired in virus-infected or tumor cells, which results in lack of engagement of inhibitory receptors and thus activation of NK cells (*1, 6*). Hence, class I serves as a positive indicator for the integrity of cells, protecting against NK cell attack. In contrast, MICA and its close relative MICB may signal cellular distress and evoke immune responses. These molecules function as stress-inducible antigens in intestinal epithelium and are recognized alike by γδ T cells with the TCR variable region $V_\delta1$ (*7, 8*). In addition, they are frequently expressed in epithelial tumors including lung, breast, kidney, ovary, prostate, and colon carcinomas (*9*). We investigated receptor interactions of MICA.

A soluble form of MICA (sMICA) including the α1α2α3 extracellular domains was expressed and purified (*10*). Addition of sMICA to cytotoxicity assays inhibited the responses of several $V_\delta1$ γδ T-cell clones to C1R cell transfectants expressing MICA (Fig. 1A) (*8, 11*). We investigated whether this effect was associated with expression of the γδ TCRs alone or involved surface molecules that occurred separately. Flow cytometry showed binding of biotinylated sMICA (bio-sMICA) to several $V_\delta1$ γδ T-cell clones (*10*). However, stainings of peripheral blood lymphocytes (PBLs) revealed binding of bio-sMICA to most γδ T cells (of the $V_\delta1$ and $V_\delta2$ subsets), $CD8^+$ T cells, and $CD56^+$ NK cells, but only to a few $CD4^+$ T cells. The cell lines NKL (NK cell) and Hut 78 (T cell) were positive, whereas CEM, Jurkat, HPB-ALL, MOLT4, and PEER (T cells), and Daudi and Raji (B cells) were negative (*10, 12*). These interactions were analyzed with monoclonal antibodies (mAbs) that were screened for binding specificities matching those of bio-sMICA (*10*). Two selected mAbs, 5C6 and 1D11, stained NKL and the $V_\delta1$ γδ T-cell clones and blocked binding of bio-sMICA (Fig. 1, C and D). As with sMICA, both mAbs inhibited T-cell recognition of MICA (Fig. 1B). With PBLs from several individuals, the distribution of epitopes recognized by these mAbs replicated the staining pattern of bio-sMICA (Fig. 2) (*10*). The mAbs 5C6 and 1D11 cross-blocked surface binding (*13*). Thus, MICA interacted with a surface receptor (MICR) that was widely distributed on lymphocyte subsets.

To identify MICR, we used representational difference analysis (RDA) (*14*). Representations of cDNAs were prepared from pools of $CD4^+$ T-cell clones that were positive or negative for MICR expression. Three rounds of hybridization-subtraction and amplification yielded a representational difference product (RDP) of five DNA fragments. Four of these probably were not relevant. The most prominent fragment matched the sequence of NKG2D, which is an orphan C-type lectin-like NK cell receptor of unknown expression and function (Fig. 3A) (*15*).

NKG2D was scrutinized as a candidate for MICR. Blot hybridization confirmed the presence of NKG2D mRNA in NKL and Hut 78 cells, as well as in a $V_\delta1$ γδ T cell line and in $CD8^+$ T cells isolated from PBLs (Fig. 3B) (*16*). A second transcript of higher molecular weight presumably corresponded to a transcriptional variant of NKG2D. In contrast, little or no mRNA was detected in Jurkat, HPB-ALL, and peripheral blood $CD4^+$ T cells. Thus, the distribution of NKG2D mRNA, which was in accord with previous limited data (*15*), matched the expression of MICR. Immunoprecipitations with mAbs 5C6 and 1D11 identified a single surface protein that was expressed on NKL and Hut 78 but not on Jurkat cells (Fig. 3C). Its apparent molecular mass of 42 kD matched

[1]Fred Hutchinson Cancer Research Center, Clinical Research Division, 1100 Fairview Avenue North, Seattle, WA 98109, USA. [2]DNAX Research Institute of Molecular and Cellular Biology, Palo Alto, CA 94304, USA.

*These authors contributed equally to this work and are listed in alphabetical order.

†Present address: Technical University of Munich, Institute of Microbiology, Trogerstrasse 32, D-81675 Munich, Germany.

‡To whom correspondence should be addressed. E-mail: tspies@fred.fhcrc.org

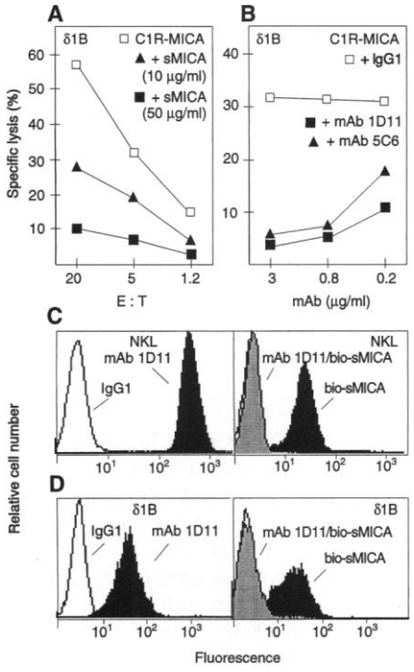

Fig. 1. Inhibition of γδ T-cell function and staining of NKL and of $V_\delta1$ γδ T cells by soluble MICA (sMICA) and mAb 1D11. (**A**) Cytotoxicity of $V_\delta1$ γδ T-cell clone δ1B (*8*) against C1R-MICA transfectants was inhibited by sMICA (*10*). (**B**) As with sMICA, mAbs 1D11 and 5C6 inhibited lysis by the δ1B T cells. Data in (A) and (B) are representative of three different $V_\delta1$ γδ T-cell clones tested. In (B), E:T was 5:1. (**C** and **D**) By indirect fluorescence and flow cytometry, mAb 1D11 stained NKL cells and δ1B T cells. Preincubation with mAb 1D11 inhibited binding of bio-sMICA detected with streptavidin-conjugated phycoerythrin (*10*). Open profiles are IgG1 control stainings. Similar results were obtained with mAb 5C6 and with the Hut 78 αβ T-cell line and two other $V_\delta1$ γδ T-cell clones.

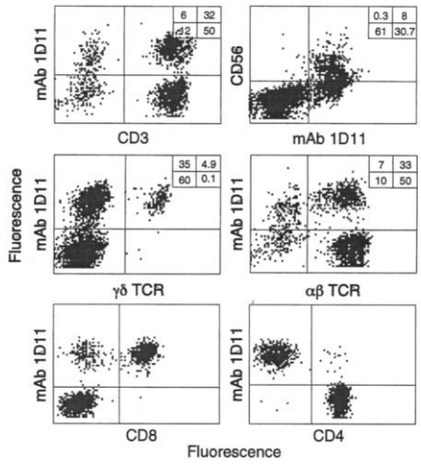

Fig. 2. Expression of a receptor for MICA on lymphocyte subsets. Two- and three-color flow cytometric analysis of freshly isolated PBLs (*10*). Upper four density plots show the indicated stainings of total PBLs; bottom two plots show stainings of gated $CD3^+$ T cells. Numbers in upper right fields indicate percentages of gated cells in quadrants. Similar results were obtained with PBLs from six healthy individuals and by using mAb 5C6. The low staining resolution in the CD56 plot was mainly due to large numbers of $CD56^{low}$ cells.

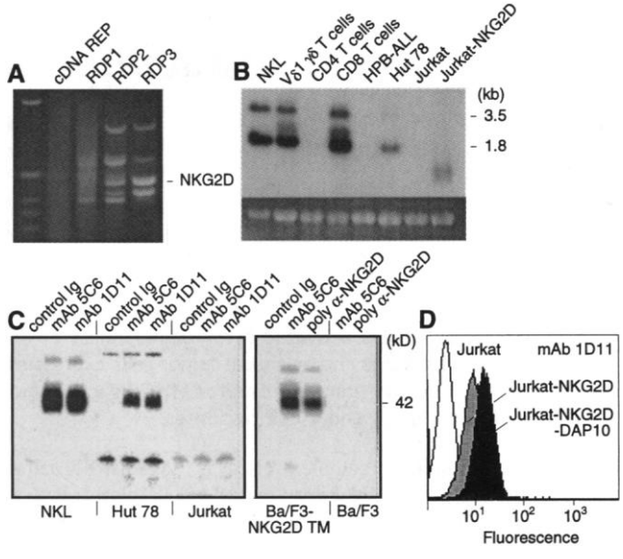

Fig. 3. NKG2D is the receptor for MICA. (**A**) Identification of NKG2D as a candidate sequence by cDNA RDA (*14*). Lanes show the Dpn II restriction enzyme representation (cDNA REP) and the sequential representational difference products (RDP1–RDP3). The NKG2D Dpn II cDNA fragment is of 430 base pairs. (**B**) A full-length NKG2D cDNA was used as a probe in blot hybridization of total RNAs from the NKL, HPB-ALL, Hut 78, and Jurkat cell lines, from a $V_\delta1$ γδ T cell line, and from $CD4^+$ and $CD8^+$ αβ T cells purified from PBLs. Presence or absence of the NKG2D mRNA of ~1.8 kb correlated with surface binding of bio-sMICA and mAbs 1D11 and 5C6 (Figs. 1 and 2; see text). The larger transcript of ~3.5 kb presumably was a transcriptional variant of NKG2D. Jurkat-NKG2D transfectants (last lane) have a shorter transcript because of their transfection with a coding region construct. Bottom of panel shows RNA sample loadings. (**C**) Immunoprecipitation of NKG2D with mAb 5C6 or 1D11 from ^{125}I-surface-labeled cell lines and from Ba/F3 cell transfectants expressing a transmembrane mutant of NKG2D in the absence of DAP10 (*17*). The protein with a molecular mass of 42 kD corresponds to NKG2D (*17*). (**D**) Flow cytometry showed binding of mAb 1D11 to the Jurkat-NKG2D transfectants but not to the untransfected cells. Binding was increased by coexpression of DAP10 (*17, 18*).

independent data obtained with mAb 5C6 and polyclonal antibodies specific for NKG2D (*17*). Transfection of Jurkat cells with NKG2D cDNA resulted in positive stainings with mAbs 5C6 and 1D11 (Fig. 3D) (*18*); the low fluorescence intensities were at least partly explained by the small amounts of NKG2D mRNA (Fig. 3B). As shown by Wu *et al.* (*17*), NKG2D forms complexes with DAP10, a membrane adaptor protein that is distantly related to DAP12 (*19*). Coexpression of DAP10 in the Jurkat-NKG2D transfectants augmented binding of mAbs 5C6 and 1D11 (Fig. 3D). Similarly increased was binding of bio-sMICA, which also bound to transfected mouse Ba/F3 cells expressing large amounts of NKG2D in the absence of DAP10 as a result of a transmembrane mutation (*13, 17*). Surface NKG2D was immunoprecipitated from these transfectants with mAb 5C6 and the antiserum to NKG2D (Fig. 3C) (*17*). These results demonstrated that NKG2D was the receptor for MICA.

NKG2D lacks a tyrosine-based inhibitory motif in its cytoplasmic tail and may function as an activating receptor (*1, 15*); signaling may be enabled by DAP10, which has an SH2 domain-binding site for the p85 subunit of phosphoinositide 3-kinase (*17*). An activating function was supported by the inhibition of γδ T-cell recognition of MICA mediated by mAb to NKG2D (anti-NKG2D) (Fig. 1B). However, these responses can also be inhibited by mAbs against γδ TCRs, implying that their activation also requires TCR engagement (*8*). To examine whether NKG2D functions in the absence of TCR, we used NK cell (NKL) effectors (*20*). These showed the expected cytotoxicity against Daudi cells, which lack β_2-microglobulin (β_2m) and thus MHC class I, whereas Daudi-β_2m transfectants were protected by the restored expression of class I; inhibition of NKL was mediated by HLA-E, the ligand for CD94-NKG2A (Fig. 4A) (*4*). However, coexpression of MICA sensitized Daudi-β_2m cells to lysis, which could be inhibited by anti-MICA (mAb 2C10) and anti-NKG2D (Fig. 4A). MICA did not diminish surface expression of class I (*13*). Hence, masking of HLA-E on Daudi-β_2m-MICA cells increased cytolysis to a level above that recorded with Daudi cells (Fig. 4A). Ligation of NKG2D on NKL with mAb 1D11 or 5C6 induced redirected lysis of Fc receptor (FcR)-bearing P815 cells, similar to the responses with anti-CD16 (Fig. 4B) (*21*). Thus, NKG2D had an activating function that was triggered by engagement of MICA. Similar

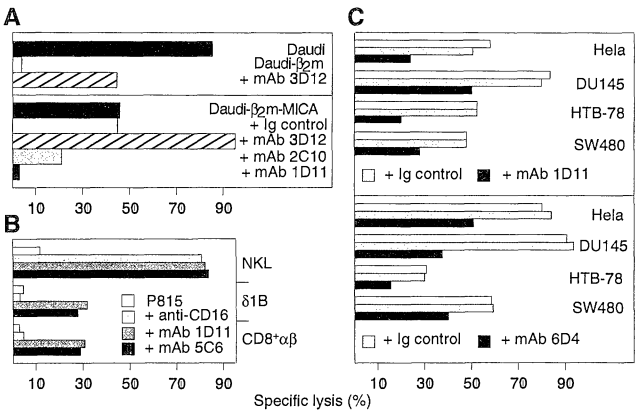

Fig. 4. Activation of effector cells by MICA engagement or ligation of NKG2D. (**A**) Expression of MICA sensitized Daudi-β_2m transfectants to lysis by NKL cells. Cytotoxicity was inhibited by anti-MICA (mAb 2C10) or anti-NKG2D (mAb 1D11). Anti-HLA-E mAb 3D12 restored lysis (*4*). (**B**) The anti-NKG2D mAbs 1D11 and 5C6 induced redirected lysis of mouse mastocytoma FcγR$^+$ P815 cells by NKL cells, by the δ1B $V_\delta1$ γδ T-cell clone, and by a peripheral blood CD8$^+$ αβ T-cell clone (*10*). Data shown are representative of four and five T-cell clones, respectively. (**C**) Cytotoxicity of NKL cells against the HeLa (cervical), DU145 (prostate), HTB-78 (ovary), and SW480 (colon) tumor cell lines was decreased by anti-NKG2D mAb 1D11 or by F(ab′)^2 fragments of the anti-MICA and anti-MICB mAb 6D4 but not by control IgG. Inhibitions were partial, as is often the case in antibody blocking. Data in (A) to (C) represent reproducible averages of three to five independent experiments and were obtained at an E:T of 10:1.

anti-NKG2D mAb-dependent cytotoxicity against P815 cells was observed with four $V_\delta1$ γδ T-cell clones tested and with five of eight NKG2D$^+$ CD8$^+$ αβ T-cell clones derived from PBLs (Fig. 4B) (*21*). Thus, in agreement with its broad distribution on most γδ T cells, CD8$^+$ αβ T cells, and NK cells, NKG2D activated or positively modulated responses by diverse effector cells.

$V_\delta1$ γδ T cells recognize MICA and MICB on epithelial tumor cell lines and on freshly isolated autologous and heterologous epithelial tumor cells (*9*). These responses were inhibited by the anti-NKG2D mAbs 5C6 and 1D11, with target cell lines derived from liver (Hep-G2), cervical (HeLa), prostate (DU145 and PC-3), ovary (HTB-78), and colon (SW480 and HCT116) carcinomas (*9, 13, 22*). Similar results were obtained with NKL cells (Fig. 4C), which were cytotoxic against the tumor cell lines, although these expressed significant amounts of MHC class I, including HLA-E (*13*). This indicated that the positive signal delivered by NKG2D could overcome inhibition by other NK cell receptors—that is, CD94-NKG2A. Tumor cell killing was decreased by the mAbs to NKG2D and by F(ab′)^2 fragments of the anti-MICA and anti-MICB mAb 6D4 (Fig. 4C). Thus, γδ T cells and NK cells were activated by the interaction of NKG2D with MICA on tumor cells. Because of the equal function of MICA and MICB in γδ T-cell assays, we infer that MICB also interacts with NKG2D (*8, 9*).

Our results define the expression and function of the NK cell receptor NKG2D and its interaction with MICA, and presumably MICB, a relationship that may or may not be exclusive. NKG2D is the most common NK cell receptor known. Although NK cells can eliminate tumor cells with loss or aberrant expression of class I, the interaction of MICA with NKG2D may promote antitumor responses in the presence of class I, depending on the balance of multiple inhibitory and activating signals, relative amounts of receptors and their ligands, and NK cell activation state (*1*). As with NK cells, $V_\delta1$ γδ T cells and CD8$^+$ αβ T cells could be activated by ligation of NKG2D; however, only the former respond against tumor cells expressing MICA or MICB, consistent with a synergistic mode of activation that may require signaling by TCRs and NKG2D (*8, 23*). Thus, the interaction of NKG2D with MICA and MICB may potentially enhance diverse antitumor innate NK cell and antigen-specific T-cell responses.

References and Notes

1. L. L. Lanier, *Annu. Rev. Immunol.* **16**, 359 (1998); W. M. Yokoyama, *Curr. Opin. Immunol.* **10**, 298 (1998).
2. M. Colonna and J. Samaridis, *Science* **268**, 405 (1995); N. Wagtmann *et al.*, *Immunity* **2**, 439 (1995).
3. C. Chang, *Eur. J. Immunol.* **25**, 2433 (1995); A. G. Brooks, P. E. Posch, C. J. Scorzelli, F. Borrego, J. E. Coligan, *J. Exp. Med.* **185**, 795 (1997).
4. V. M. Braud *et al.*, *Nature* **391**, 795 (1998); N. Lee *et al.*, *Proc. Natl. Acad. Sci. U.S.A.* **95**, 5199 (1998).
5. J. H. Phillips, J. E. Gumperz, P. Parham, L. L. Lanier, *Science* **268**, 403 (1995); I. Carena, A. Shamshiev, A. Donda, M. Colonna, G. De Libero, *J. Exp. Med.* **186**, 1769 (1997); H. Ikeda *et al.*, *Immunity* **6**, 199 (1997); C. Noppen *et al.*, *Eur. J. Immunol.* **28**, 1134 (1998).
6. K. Karre, H. G. Ljunggren, G. Piontek, R. Kiessling, *Nature* **319**, 675 (1986).
7. V. Groh *et al.*, *Proc. Natl. Acad. Sci. U.S.A.* **93**, 12445 (1996).
8. V. Groh, A. Steinle, S. Bauer, T. Spies, *Science* **279**, 1737 (1998).
9. V. Groh *et al.*, *Proc. Natl. Acad. Sci. U.S.A.* **96**, 6879 (1999).
10. sMICA was prepared as described [S. Bauer, S. T. Willie, T. Spies, R. K. Strong, *Acta Crystallogr. D* **54**, 451 (1998)]. For biotinylation, we treated sMICA (1 mg/ml) with EZ-Link-Sulfo-NHS-LC-Biotin (Pierce) at a molar ratio of 1:7 for 30 min at 37°C. After purification on Bio-Gel P60 (Bio-Rad), we tested biotinylation by preadsorption with avidin-Sepharose and SDS–polyacrylamide gel electrophoresis. For stainings, cells in 0.1 ml of buffer were incubated with bio-sMICA (3 μg) for 1 hour at 4°C, pelleted, and treated with streptavidin-phycoerythrin (4 μg/ml) (Molecular Probes) for 30 min at 4°C. We examined washed and fixed cells (1% paraformaldehyde) by flow cytometry. Cell lines were from the American Type Culture Collection (ATCC). The $V_\delta1$ γδ T cell clones and NKL cells have been described (*8, 20*). For Fig. 2, PBLs were isolated by using Ficoll/Hypaque, stained with fluorochrome-conjugated mAbs [anti-CD3, anti-CD4, anti-CD8, anti-CD56, anti-TCR-α/β-1 (Becton-Dickinson), and anti-human pan TCRγδ (Endogen)], and examined by two- or three-color flow cytometry. We detected binding of mAb 1D11 with phycoerythrin-conjugated goat F(ab′)^2 antibody to mouse immunoglobulin (Biosource). We generated mAbs 5C6 and 1D11 (IgG2a and IgG1 isotypes, respectively) by immunization of RBF/DnJ mice (Jackson Laboratories) with NKL cells as described (*7*). We screened hybridoma supernatants for staining of NKL and $V_\delta1$ γδ T cells and for inhibition of binding of bio-sMICA and of NKL cytotoxicity against C1R-MICA targets.
11. Chromium release assays and mAb inhibition experiments were as described (*8*). In Fig. 1A, sMICA was added at the indicated concentrations to target cells before they were plated onto T cells.
12. S. Bauer, unpublished data.
13. V. Groh, unpublished data.
14. RDA was done as described [M. Hubank and D. G. Schatz, *Nucleic Acids Res.* **22**, 5640 (1994); N. Lisitsyn, N. Lisitsyn, M. Wigler, *Science* **259**, 946 (1993)]. RNAs for tester and driver cDNA samples were prepared with STAT-60 reagent (Tel-Test) from pools of CD4$^+$ T-cell clones that were positive and negative, respectively, for binding of mAb 1D11 and were obtained by sorting from PBLs; polyadenylated mRNA was isolated with an Oligotex Combi kit (Quiagen), and Super Script (Gibco BRL) was used to synthesize cDNA. Dpn II representations were subjected to three rounds of hybridization, ligation with adaptor oligonucleotides, and amplification. The indicated fragment in RDP3 was a 430-base-pair sequence of NKG2D (*15*).
15. J. P. Houchins, T. Yabe, C. McSherry, F.-H. Bach, *J. Exp. Med.* **173**, 1017 (1991); T. Yabe *et al.*, *Immunogenetics* **37**, 455 (1993).
16. Total RNAs were prepared and blot hybridized as described (*7*). The CD4$^+$ and CD8$^+$ T cells were positively selected from PBLs by using antibody-coated magnetic beads (Milteny Biotech).
17. J. Wu *et al.*, *Science* **285**, 730 (1999).
18. We transfected Jurkat cells with NKG2D and DAP10 (*17*) cDNA expression constructs in pcDNA3.1/Neo or pcDNA3.1/Hygro (Invitrogen) as described [A. G. Grandea, M. J. Androlewicz, R. S. Athwal, D. E. Geraghty, T. Spies, *Science* **270**, 105 (1995)]. We obtained the full-length NKG2D coding sequence by reverse transcription–polymerase chain reaction using NKL cell mRNA and oligonucleotide primers with flanking Bam HI or Sal I restriction site sequences.
19. L. L. Lanier, B. Corliss, J. Wu, J. H. Phillips, *Immunity* **8**, 693 (1998).
20. M. J. Robertson *et al.*, *Exp. Hematol.* **24**, 406 (1996).
21. Redirected lysis assays with ^{51}Cr-labeled P815 targets were standard cytotoxicity assays in the presence of anti-CD16 (mAb 3G8; Immunotech) or anti-NKG2D mAb 5C6 or 1D11, each at 5 μg/ml. The effector-to-target cell ratios (E:T) in Fig. 4 were 10:1. Ig-isotype controls used in all experiments. The CD8$^+$ αβ T-cell clones used in Fig. 4B were obtained by sorting with anti-CD8 (Becton-Dickinson) from PBLs and were grown under the same conditions as the $V_\delta1$ γδ T cells (*8*).
22. The epithelial tumor cell lines were from the American Type Culture Collection.
23. Inhibition by anti-γδ TCR mAb of epithelial tumor cell lysis by $V_\delta1$ γδ T cells has been reported by Maeurer *et al.* [*J. Exp. Med.* **183**, 1681 (1996)].

24. Supported by the Deutsche Forschungsgemeinschaft (S.B.) and NIH grants PO1 CA18221 and RO1 AI30581. DNAX is supported by Schering Plough Corporation. We thank D. Morris, S. Willie, and R. Strong for help in the production and purification of sMICA; R. Rhinehart for technical assistance; D. Geraghty for mAb 3D12; M. Robertson for the NKL cell line; D. Schatz for the RDA protocol; and A. Grandea for suggestions.

14 April 1999; accepted 24 June 1999